

## **A SIMPLE APPROACH TO THE LARGE-DISPLACEMENT ANALYSIS OF ELASTIC FRAMED STRUCTURES**

Giovanni Facchin<sup>1</sup>, Alfonso Nappi<sup>2</sup>, Daniele Zaccaria<sup>3</sup>

<sup>1</sup>Research Assistant, <sup>2</sup>Professor, <sup>3</sup>Associate Professor

Department of Engineering and Architecture

University of Trieste, P.le Europa 1, 34127 Trieste, Italy

nappi@units.it

## Abstract

The paper is centered on an iterative procedure, which can be adopted for the structural analysis of elastic frames subjected to large displacements. In consequence, the equilibrium equations are written by considering the deformed configuration.

The algorithm is based on the finite element method and essentially requires the solution of a sequence of linear elastic problems. At each iteration, the nodal displacements are updated according to the *small displacement theory*. Thus, the numerical approach discussed here makes use of the usual tools, which are typical of a simple linear elastic analysis. More specifically, after a preliminary analysis that is performed by considering a given set of external loads and by imposing equilibrium with respect to the initial configuration, the actual curvatures of the beam elements are determined and convenient equivalent nodal loads are computed. Next, a new mesh is generated in order to account for the deformed configuration of the framed structure and further incremental displacements are found by applying a set of nodal loads, which represent the difference between the given loads and the loads determined at the end of the previous analysis. The process continues until a convenient *measure* of the discrepancy between the displacements computed at the last iteration and the displacements estimated at the previous iteration is below a given tolerance. To this aim, it is possible to compare the Euclidean norms of the displacement vectors evaluated at two subsequent iterations.

Some preliminary numerical tests on simple plane systems show that the approach presented in this paper does give results, which are consistent with analytical and/or experimental solutions.

**Keywords:** Convergence, Discrete model, Finite element method, Framed structures, Linear-elastic analysis, Iterative schemes, Large displacements, Structural instability.

## 1. Introduction

The topic of this paper is related to the field of structural systems, which are subjected to large displacements and must be studied by writing the equilibrium equations with reference to deformed configurations. The research work in this area has been quite extensive [1] and ranges from cable structures [2] to fluid-structure interaction [3, 4], from creep buckling of framed structures [5] to structural dynamics [6], from systems characterized by prismatic joints [7] to elastic-plastic structures [8].

More specifically, this work is concerned with the numerical analysis of framed structures, which have led to the development of several sophisticated analytical and numerical methods [9 – 13]. Here, we focus on a simple computer method, which essentially makes use of numerical tools, which were developed in the context of the *small-displacement theory* and have already been applied to space structures subjected to uniaxial stress states [14, 15].

This approach requires an iterative scheme that is based on the solution of a sequence of linear equations, which are derived by considering discrete finite element models in the context of the *small-displacement theory*. Namely, for a given set of input variables (external loads and/or imposed displacements), a solution is found by considering a traditional finite element mesh and by imposing the equilibrium with reference to the initial configuration, as typical of the *small-*

*displacement theory*. Next, the internal *generalized forces* (actual forces and moments) are computed by considering the present deformed configuration (*i.e.*, in accordance with the *large-displacement theory*) and an updated mesh is generated in order to take into account the new geometry of the structural system. At this stage, incremental displacements are computed (again on the basis of the *small-displacement theory*) by applying equivalent nodal loads, which represent the difference between the initial (given) loads and the nodal loads in equilibrium with the current internal *generalized forces*. The process continues until the algorithm eventually converges toward the correct solution.

As discussed below, each new mesh is generated by exploiting traditional concepts that are currently adopted in the context of *isoparametric finite elements* and a convenient stiffness matrix has been developed with the aim of obtaining equivalent nodal loads that (for a given set of virtual displacements) do the same work, which is done by the internal *generalized forces*.

So far, basic beam elements characterized by two nodes (*i.e.*, six degrees of freedom) and suitable for the analysis of plane systems have been considered. However, despite this limitation and the extreme simplicity of the approach (in terms of theoretical fundamentals and computational tools), a few preliminary sample problems tend to show that accurate solutions can be found.

## 2. The numerical model

The first step requires a traditional mesh developed for plane frames by using beam elements. So far, only 2-node finite elements have been considered. For any given set of external loads and/or imposed displacements, a numerical solution is immediately determined in accordance with the *small-displacement theory*. Namely, we easily find a displacement vector  $U_0$ , which gives the nodal *generalized displacements*, referred to a set of global coordinates  $x$ - $y$ .

With reference to the same global coordinates, the displaced position of each node will be given by the pair  $x_n$ - $y_n$ . In addition, a rotation  $\vartheta_n$  shall be considered for every node. However, for each element, it is also possible to introduce a local axis  $\psi$  (with its origin in the first node), which passes through the second node. Since 2-node beam elements are characterized by cubic shape functions, typical configurations can be the ones depicted in Fig. 1.

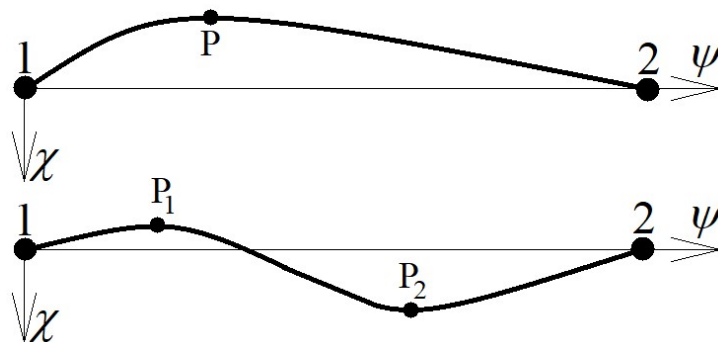


Figure 1: Typical deformed configurations for 2-node beam elements

On the basis of the same path of reasoning that is followed in the field of *isoparametric elements*, the coordinates  $\chi(\psi)$  of each point of the geometrical axis of the beam can be found by introducing

cubic shape functions (the same functions utilized for displacements along the  $\chi$ -direction). Thus, we can define a function  $\chi(\psi)$  that depends on the coordinates  $\chi_1$  and  $\chi_2$  (which are obviously equal to zero in this context), and on the slopes  $\mathcal{G}_1$  and  $\mathcal{G}_2$ .

At this stage, for each element it is necessary to compute convenient *generalized nodal loads* that correspond to the displaced configuration. To this aim, we can start by determining the curvatures at the nodes, say  $c = \chi''/(1+\chi'^2)^{2/3}$ , where  $\chi' = d\chi(\psi)/d\psi$  and  $\chi'' = d^2\chi(\psi)/d\psi^2$ . The product between these curvatures and the bending stiffness  $EI$  gives the moments at the end nodes (where  $E$  denotes Young's modulus and  $I$  the moment of inertia). Then, the forces acting along the  $\chi$ -direction can be found by imposing equilibrium. As to the forces acting along the  $\psi$ -direction, they can be computed by considering the strain  $\varepsilon$  at a point such as P in the upper part of Fig. 1, or the average strain  $\varepsilon_a$  at points such as P<sub>1</sub> and P<sub>2</sub> in the lower part of the same figure. Eventually, we can multiply  $\varepsilon$  or  $\varepsilon_a$  by the axial stiffness  $EA$  in order to obtain the required forces (where  $A$  represents the area of the cross section).

Once we have the *generalized nodal loads* in each element, we can define the vector of the nodal loads concerned with the entire structure (say  $\mathbf{Q}^*$ ) and determine the load vector  $\Delta\mathbf{Q}^*$ , which represents the difference between  $\mathbf{Q}^*$  and the given loads (say  $\mathbf{Q}$ ).

Now, it is possible to activate an iterative process in order to end up with a displaced configuration for which the difference  $\Delta\mathbf{Q}^*$  becomes negligible. This aim can be achieved by following a procedure already developed for the analysis of structural systems, which are only subjected to axial forces [14, 15].

To do so, we need to generate an updated mesh that is representative of the current configuration. Therefore, we can make use of 2-node finite elements whose geometrical axes are defined by the functions  $\chi(\psi)$  discussed above. Since the iterative process requires the solutions of structural problems according to the *small-displacement theory*, the stiffness matrix of the beam elements can be defined by exploiting the *principle of virtual works*.

First of all, we observe that, in the presence of incremental quantities and linear-elastic material response, the stiffness matrix of the finite element allows one to establish a linear relationship between an incremental displacement vector  $\Delta\mathbf{u}$  and an incremental load vector  $\Delta\mathbf{q}$ . In this context,  $\Delta\mathbf{u}$  and  $\Delta\mathbf{q}$  will be defined with reference to the local axes  $\psi$ - $\chi$ . Let us now denote the components of  $\Delta\mathbf{u}$  by the symbols  $\Delta u_1, \Delta v_1, \Delta \mathcal{G}_1, \Delta u_2, \Delta v_2, \Delta \mathcal{G}_2$ . Similarly, the symbols  $\Delta q_1, \Delta f_1, \Delta m_1, \Delta q_2, \Delta f_2, \Delta m_2$  can be used to define the corresponding scalar components of  $\Delta\mathbf{q}$ .

After replacing the function  $\chi(\psi)$  with a convenient function  $\chi(\xi)$ , in which  $\xi$  denotes the traditional non-dimensional coordinate  $\xi$ , whose value ranges between -1 and 1, we can define the axial force  $\Delta N_1(\xi)$  and the moment  $\Delta M_1(\xi)$  that would be given by the *generalized nodal loads*  $\Delta q_1, \Delta f_1$  and  $\Delta m_1$  if the second end of the element were clamped. Therefore,  $\Delta N_1(\xi)$  and  $\Delta M_1(\xi)$  are determined with reference to the configuration defined by the function  $\chi(\xi)$ , which represents the initial, non-deformed configuration at the beginning of the first iteration.

If  $2\ell$  is the length of the geometrical axis in the displaced (usually curved) configuration, we easily derive the elongation  $dn_1 = \Delta N_1(\xi) \ell d\xi/(EA)$  and the rotation  $d\mathcal{G}_1 = \Delta M_1(\xi) \ell d\xi/(EI)$  concerned with a beam element whose length is  $\ell d\xi$ .

Then, we can focus on three different load conditions (say,  $C1, C2, C3$ ) by considering the *generalized forces*  $q_1=1, f_1=1$  and  $m_1=1$  at the first node. In consequence, we will find the axial

forces  $N_{C1}(\xi)$  and  $N_{C2}(\xi)$  that are given by the forces  $q_1=1$  and  $f_1=1$ , as well as the moments  $M_{C1}(\xi)$ ,  $M_{C2}(\xi)$  and  $M_{C3}(\xi)=1$  that are induced by the *generalized forces*  $q_1=1, f_1=1$  and  $m_1=1$ .

Now, it is possible to apply the *principle of virtual works* by separately considering the effects of the load conditions  $C1, C2, C3$  and by imposing three different sets of *generalized displacements* at the first node of the beam element:  $\Delta \hat{\mathbf{u}}_\alpha=[1 \ 0 \ 0]^T$ ,  $\Delta \hat{\mathbf{u}}_\beta=[0 \ 1 \ 0]^T$ ,  $\Delta \hat{\mathbf{u}}_\gamma=[0 \ 0 \ 1]^T$ . In other words, the vector  $\Delta \hat{\mathbf{u}}_s$  ( $s=\alpha, \beta, \gamma$ ) collects given values of the *generalized displacements*  $\Delta u_1, \Delta v_1, \Delta \mathcal{G}_1$ .

In the end, we obtain the internal virtual works:

$$\delta \mathcal{L}_{C1} = \delta \mathcal{L}_{C1}(\Delta q_1, \Delta f_1, \Delta m_1, q_1=1) = \int N_{C1}(\xi) \, dn_1 + \int M_{C1}(\xi) \, d\mathcal{G}_1 \quad (1a)$$

$$\delta \mathcal{L}_{C2} = \delta \mathcal{L}_{C2}(\Delta q_1, \Delta f_1, \Delta m_1, f_1=1) = \int N_{C2}(\xi) \, dn_1 + \int M_{C2}(\xi) \, d\mathcal{G}_1 \quad (1b)$$

$$\delta \mathcal{L}_{C3} = \delta \mathcal{L}_{C3}(\Delta q_1, \Delta f_1, \Delta m_1, m_1=1) = \int M_{C3}(\xi) \, d\mathcal{G}_1 \quad (1c)$$

where the integrals are to be evaluated for  $\xi$  ranging between -1 and 1. Note that the non-dimensional coordinate  $\xi$  was introduced in order to compute the integrals by means of the *Gauss method*, which requires the value of the integrand function at a given number of points (the so-called *Gauss points*) and is based on the equation

$$\int_{-1}^1 f(\xi) \, d\xi = \sum_i f(\xi_i) w_i \, d\xi \quad (2)$$

Here,  $f(\xi)$  denotes the integrand function at the  $i$ -th *Gauss point*, while  $w_i$  is a convenient weight associated to the same point. Incidentally, we made use of eleven *Gauss points* for the numerical examples reported in the next Section.

Finally, it is possible to solve three sets of three linear equations (in which  $\Delta q_1, \Delta f_1$  and  $\Delta m_1$  represent the unknowns) by imposing

- $\delta \mathcal{L}_{C1}=1, \delta \mathcal{L}_{C2}=0, \delta \mathcal{L}_{C3}=0$  when  $\Delta \hat{\mathbf{u}}=\Delta \hat{\mathbf{u}}_\alpha$
- $\delta \mathcal{L}_{C1}=0, \delta \mathcal{L}_{C2}=1, \delta \mathcal{L}_{C3}=0$  when  $\Delta \hat{\mathbf{u}}=\Delta \hat{\mathbf{u}}_\beta$
- $\delta \mathcal{L}_{C1}=0, \delta \mathcal{L}_{C2}=0, \delta \mathcal{L}_{C3}=1$  when  $\Delta \hat{\mathbf{u}}=\Delta \hat{\mathbf{u}}_\gamma$ .

In consequence, we derive the *generalized forces*  $\Delta q_1, \Delta f_1$  and  $\Delta m_1$ , which are generated at the first node when all the components of  $\Delta \mathbf{u}$  are zero, with the exception of  $\Delta u_1=1$  or  $\Delta v_1=1$  or  $\Delta \mathcal{G}_1=1$ . As a matter of fact, when  $\Delta u_1$  is the only non-zero *generalized displacement*,  $q_1=1$  is the only *generalized force* that does a non-zero external virtual work (namely, a *unit work*, since  $\Delta u_1$  is also equal to 1). Similarly,  $f_1=1$  and  $m_1=1$  are the only *generalized forces* that do a non-zero (unit) external virtual work, when  $\Delta v_1$  or  $\Delta \mathcal{G}_1$  is the only non-zero *generalized displacement*.

This means that we have actually determined the entries  $k_{ij}$  of the stiffness matrix  $\mathbf{k}$  (with  $i, j=1, 2, 3$ ), since the generic entry  $k_{ij}$  denotes the  $i$ -th entry of  $\Delta \mathbf{q}$  when all the entries of  $\Delta \mathbf{u}$  are zero, with the exception of  $j$ -th entry, which must attain a unit value.

Then, it is possible to immediately compute the entries  $k_{ij}$  (with  $i=4, 5, 6$  and  $j=1, 2, 3$ ), in view of the equations  $\Delta q_2=-\Delta q_1$  and  $\Delta f_2=-\Delta f_1$ , while  $\Delta m_2$  must be in equilibrium with  $\Delta m_1$  and the moment corresponding to the couple  $\Delta f_1, \Delta f_2$ .

Of course, an analogous procedure allows one to determine the entries  $k_{ij}$ , with  $i=1, \dots, 6$  and  $j=4, 5, 6$ . Indeed, we only need to clamp the first node, consider the axial force  $\Delta N_2(\xi)$  and the

bending moment  $\Delta M_2(\xi)$  induced by the *generalized nodal loads*  $\Delta q_2$ ,  $\Delta f_2$  and  $\Delta m_2$ , and apply the *principle of virtual works* by imposing that every *generalized displacement* is zero with the exception of  $\Delta u_2=1$  or  $\Delta v_2=1$  or  $\Delta \theta_2=1$ .

After computing the stiffness matrix of each element, it is possible to derive the usual linear system  $\mathbf{K} \Delta \mathbf{U} = \Delta \mathbf{Q}$ , where  $\Delta \mathbf{U}$  and  $\Delta \mathbf{Q}$  collect all the *generalized nodal displacements* and *generalized nodal forces* (both referred to the global coordinates  $x$ - $y$ ).

Therefore, by setting  $\Delta \mathbf{Q} = -\Delta \mathbf{Q}^*$ , we tend to force a solution, which is in equilibrium with the given load vector  $\mathbf{Q}$ . In fact, after solving the linear system  $\mathbf{K} \Delta \mathbf{U} = \Delta \mathbf{Q}$ , we find the incremental displacements  $\Delta \mathbf{U}$  according to the *small-displacement theory* and determine an *enhanced* displaced configuration, which is defined through the updated displacement vector  $\mathbf{U} = \mathbf{U}_0 + \Delta \mathbf{U}$ .

Then, we can define a new vector  $\Delta \mathbf{Q}^*$  and a new stiffness matrix  $\mathbf{K}$  by introducing a function  $\chi(\psi)$  or  $\chi(\xi)$  for each element, whose stiffness matrix  $\mathbf{k}$  must be updated as explained above.

Thus, it is possible to proceed with the second iteration and the iterative scheme continues until a convenient norm of  $\Delta \mathbf{Q}^*$  and/or  $\Delta \mathbf{U}$  is below a given tolerance. For the numerical tests discussed in the next Section, we imposed  $|\Delta \hat{\mathbf{U}}| / |\hat{\mathbf{U}}| < \eta$ , where  $|\cdot|$  denotes the Euclidean norm of the quantity  $[\cdot]$ ,  $\Delta \hat{\mathbf{U}}$  represents the last vector of incremental displacements,  $\hat{\mathbf{U}}$  is the vector of total (cumulative) displacements at the end of the previous iteration and  $\eta$  refers to the selected threshold.

### 3. Numerical tests

In order to check the numerical approach discussed above, we carried out some preliminary tests, which were concerned with structural systems characterized by a simple geometry. A parameter  $\eta = 10^{-18}$  was chosen to end the iterative procedure.

We started by considering a highly flexible cantilever beam subjected to a vertical load  $Q$  at the free end (Fig.2). By using a discrete model consisting of ten elements, the vertical and horizontal displacements (at the end of the iterative process) turned out to be nearly 30% and 5% of the beam length. As for the load, we assumed  $Q = 0.5$  units and the absolute values of the *generalized nodal forces* that should have been zero turned out to be in the range  $2.7 \cdot 10^{-15} \div 1.5 \cdot 10^{-11}$  units. Similarly, the vertical force and the moment at the clamped end, which were determined by taking into account the displaced configuration, satisfied the equilibrium conditions in an excellent way. Indeed, the difference between the moment due to the external load and the moment computed at the constrained node was less than  $3.5 \cdot 10^{-14}$  units.

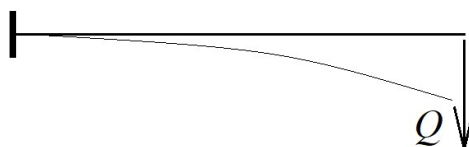


Figure 2: Cantilever beam

A second example was also concerned with a single structural member. In this case, we focused on the classical problem of the post-buckling behavior of a simply supported beam subjected to a compressive load  $Q$  (cf. Fig. 3). For given values of  $L$  (beam length),  $I$  (moment of inertia) and  $E$

(Young’s modulus), it is possible to express  $Q$  as a function of the angle  $\alpha$  and/or the mid-point deflection  $\delta$ . For instance, as shown, e.g., in Ref. [16], we can derive the relationship

$$Q = 4 K^2 EI / L^2 \tag{3}$$

where  $K$  is a complete elliptic integral of the first kind. Therefore, the load  $Q$  depends on the rotation  $\alpha$ . In fact, by introducing the parameter  $\beta = \sin(\alpha/2)$ ,  $K$  can be written on the basis of the classical notations due to Legendre (first integral in the following equation) and Jacobi (second integral):

$$K = \int_0^{\pi/2} (1 - \beta^2 \sin^2 \varphi)^{-1/2} d\varphi = \int_0^1 (1 - y^2)^{-1/2} (1 - \beta^2 y^2)^{-1/2} dy \tag{4}$$

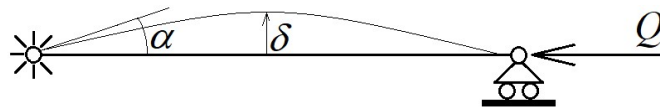


Figure 3: Simply supported beam subjected to a compressive load

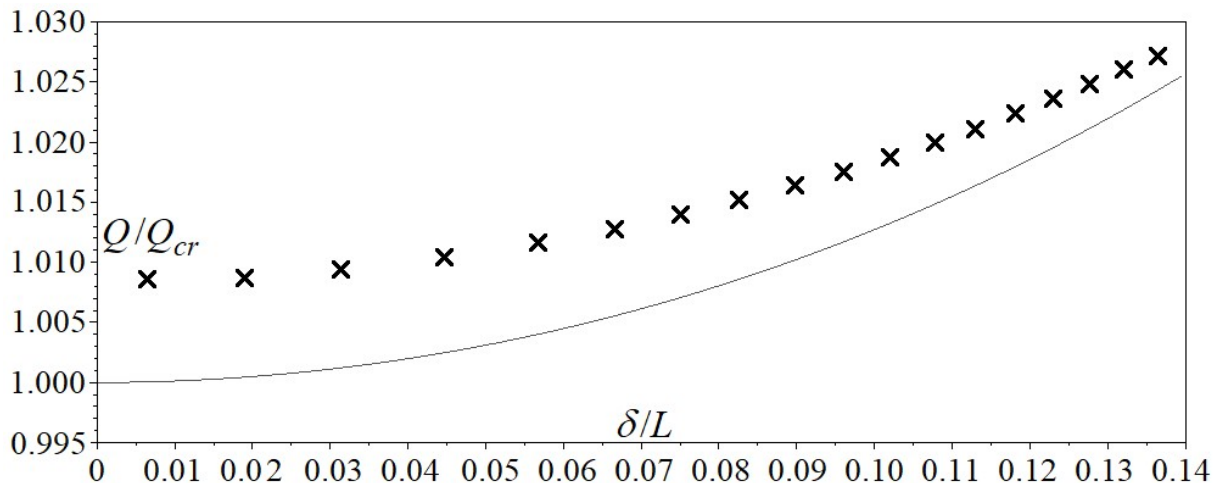


Figure 4: Analytical and numerical post-buckling response

Clearly, in both cases we have a function  $K=K(\alpha)$  and, hence,  $Q=Q(\alpha)$ .

Alternatively, it is possible to obtain the equation  $Q=4\beta^2 EI / \delta^2$ , which eventually allows one to establish a relationship between the load  $Q$  and the mid-point deflection  $\delta$ .

In order to test the numerical procedure discussed here, we considered the elastic beam of Fig. 3 with  $L=1$  m,  $E=200,000$  MPa and a rectangular cross section, whose sides were 10 and 12 mm, respectively. In consequence, we obtained  $I=1,440$  mm<sup>4</sup>, which implied a critical load  $Q_{cr}=\pi^2 EI/L^2=2,842.45$  N.

Fig. 4 compares the analytical post-buckling response of the beam with the numerical solution given by a ten-element mesh. The solid curve shows the trend of the non-dimensional parameter

$Q/Q_{cr}$  as a function of  $\delta L$  according to the above equations, while the crosses correspond to the numerical results, which were obtained by imposing an increasing displacement to the free end. In order to enforce buckling, an initial vertical load was imposed (and next removed, at the beginning of the iterative procedure).

Thanks to the scale of the ordinates, it can be easily noticed that the errors are always less than 1% and tend to decrease when the load  $Q$  is increased. More specifically, when  $\delta L \approx 0.135$ , the ratio  $Q/Q_{cr}$  exceeds 1.024 in the case of the analytical solution and remains below 1.028 according to the finite element model. In consequence, the error is less than 0.4%. Instead, for low values of the ratio  $\delta L$ , it can be immediately checked that the error is in the range 0.8÷0.9%.

It should also be noted that the absolute values of the *generalized nodal forces* that should have been zero were in the range  $2 \cdot 10^{-6} \div 3 \cdot 10^{-4}$  N at the end of the final time step.

The last example is concerned with another system characterized by unstable behavior. In this case, we considered a cantilever beam connected to another beam through a slider. The second end of this beam was also constrained by a slider (Fig. 5) and was free to move to the right or to the left.

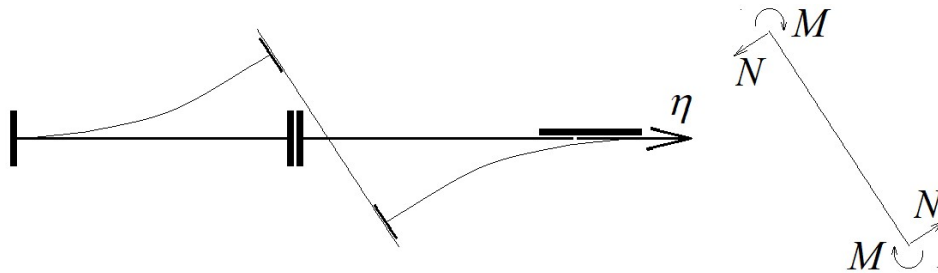


Figure 5: Structural system subjected to unstable behaviour in the presence of tensile stresses

If this structural system is subjected to tensile stresses when a horizontal displacement is imposed to the right end, it can be shown that a critical load exists, beyond which the solution characterized by a straight displaced configuration becomes unstable [17]. Thus, the right end of the first beam tends to move upwards (or downwards), while the left end of the second beam tends to move in the opposite direction. As for the load, it tends to decrease when the imposed displacement is increased, as shown by the solid line in Fig. 6.

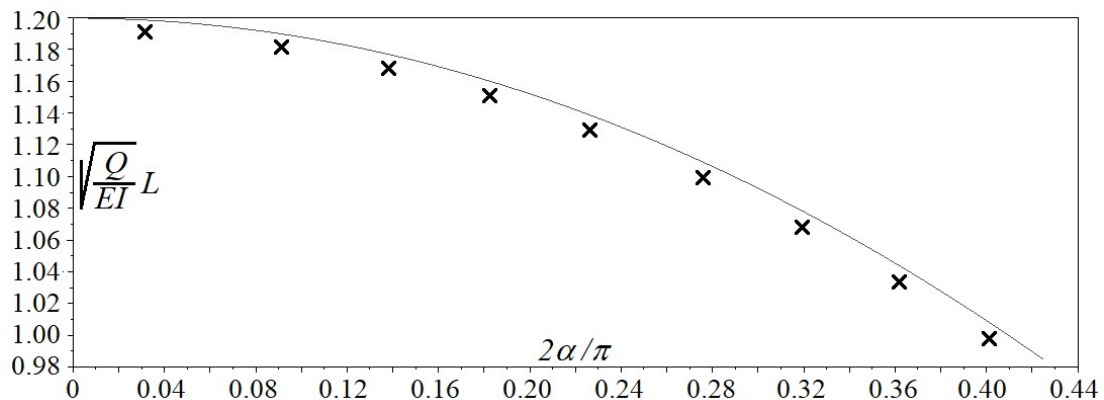


Figure 6: Analytical and numerical response of the structural system in Fig. 5

The same cross sectional area and the same length, say  $L$ , were assumed for both beams, and each structural member was discretized by using eight elements. Fig. 6 compares some numerical results (denoted by crosses) with the analytical response, which can be determined as explained in Ref. 17. As usual, the product  $EI$  denotes the bending stiffness of the beams, while  $\alpha$  represents the rotation of the slider that connects the two structural members. As suggested by the schematic view on the right-hand side of Fig. 5, the solution was found by imposing that the slider in the middle was in equilibrium (*i.e.*, by imposing that the couple induced by the normal forces  $N$  was in equilibrium with the moments  $M$  in the displaced configuration). In addition, two initial vertical loads (one upward, one downward) were imposed at the joint, with the aim of enforcing a displaced configuration. By following the same approach adopted in the case of buckling, these loads were removed at the beginning of the iterative procedure.

The plots in Fig. 6 show that the errors tend to be less than 1% even for values of  $\alpha$  that exceed  $36^\circ$  (or  $\pi/5$  radians).

#### 4. Closing remarks

An algorithm has been discussed, which is suitable for the numerical analysis of elastic plane frames subjected to large displacements. The proposed method is based on an iterative procedure, which has the advantage of requiring the traditional tools applied to the analysis of the structural systems that can be studied in accordance to the *small-displacement theory*. Therefore, a computer code can be easily implemented, even if there is a cost to be paid: the stiffness matrix of the frame must be evaluated/updated at each iteration.

In this paper, the finite element method has been used and non-traditional beam elements have been considered in order to describe the current frame geometry during the iterative process. In this way, also the classical 2-node elements succeed in taking into account curved geometrical axes. Meanwhile, the relevant stiffness matrices have been defined with the aim of obtaining equivalent nodal loads, which (for any set of virtual displacements allowed by the shape functions) do an external virtual work that equals the internal virtual work.

In order to test the potential efficiency of the algorithm, some preliminary tests have been carried out. Owing to the simple geometry of the structural systems that have been considered so far, it is probably too early to come to a definite assessment about the real performance of the finite element application presented here, but some significant comparisons with analytical solutions show that accurate results can be obtained in spite of the extreme simplicity of the numerical approach.

#### 5. References

- [1] K. Meguro, H. S. Tagel-Din, Applied Element Method Used for Large Displacement Structural Analysis, *Journal of Natural Disaster Science*, 24, 1, 25-34, 2002.
- [2] N. Zivaljic, A. Mihanovic, B. Trogrlic, Large Displacements in Nonlinear Numerical Analyses for Cable Structures, *Third European Conference on Computational Mechanics*, 128, 2006.
- [3] K. Stein, T. Tezduyar, R. Benney, Mesh Moving Techniques for Fluid-Structure Interactions With Large Displacements, *ASME Journal of Applied Mechanics*, 70, 58-63, 2003.

- [4] T.M. van Opstal, E.H. van Brummelen, A Finite-Element/Boundary-Element Method for Large-Displacement Fluid Structure Interaction with Potential Flow, *Comput. Methods Appl. Mech. Engng.*, 266, 57-69, 2013.
- [5] G. Turkalj, D. Lanc, J. Brnic, Large Displacement Beam Model For Creep Buckling Analysis Of Framed Structures, *International Journal of Structural Stability and Dynamics*, 9, 61, 2009.
- [6] S. Triantafyllou, V. Koumouisis, Small and Large Displacement Dynamic Analysis of Frame Structures Based on Hysteretic Beam Elements, *J. Eng. Mech.*, 138, 1, 36-49, 2012.
- [7] X. Tang, A Large-Displacement 3-DOF Flexure Parallel Mechanism with Decoupled Kinematics Structure, *IEEE/RSJ International Conference on Intelligent Robots and Systems*, Beijing, 9-15 Oct. 2006.
- [8] Y. Dongquan, P. Hong, Elasto-Plastic Analysis of Frame Structures under Large Displacement-Rotation Deformations, *Advanced Materials Research*, 243-249, 5968-5974, 2011.
- [9] K. J. Bathe, S. Bolourchi, Large Displacement Analysis of Three-Dimensional Beam Structures, *International Journal for Numerical Methods in Engineering*, 14, 961-986, 1979.
- [10] J. L. Meek, S. Loganathan, Large Displacement Analysis of Space-Frame Structures, *Computer Methods in Applied Mechanics and Engineering*, 72, 1, 57-75, 1989.
- [11] G. Turkalj, J. Brnic, J. Prpic-Orsic, ESA Formulation for Large Displacement Analysis of Framed Structures with Elastic-plasticity, *Computers & Structures*, 82, 23-26, 2001-2013, 2004.
- [12] D. Lanc, G. Turkalj, J. Brnic, Large-Displacement Analysis of Beam-type Structures Considering Elastic-plastic Material Behavior, *Materials Science and Engineering: A*, 499, 1-2, 142-146, 2009.
- [13] N. D. Kien, A Timoshenko Beam Element for Large Displacement Analysis of Planar Beams and Frames, *Int. J. Str. Stab. Dyn.*, 12, 2012.
- [14] G. Facchin, A. Nappi, D. Zaccaria, An Iterative Procedure for the Analysis of Nonlinear Elastic Systems Subjected to Uniaxial Loading and Large Displacements, *Civil Engineering and Architecture*, 3, 5, 153-162, 2015.
- [15] G. Facchin, A. Nappi, D. Zaccaria, Convergence Properties of an Algorithm for the Large-displacement Analysis of Elastic-plastic Space Structures, *IJRDO-Journal of Mechanical and Civil Engineering*, 2, 11, 2016.
- [16] A. Chajes, *Principles of Structural Stability Theory*, Prentice-Hall, Englewood Cliffs, NJ, 1974.
- [17] D. Zaccaria, D. Bigoni, G. Noselli, D. Misseroni, Structures buckling under tensile dead load, *Proc. R. Soc. A*, 467, 1686-1700, 2011.